

# A study on non-destructive measurement using Prompt Gamma-ray Analysis of chloride profile in concrete

I. Ujike, S. Okazaki & M. Yamate

*Graduate School of Science and Engineering, Ehime University, Matsuyama, Japan*

H. Matsue

*Japan Atomic Energy Agency, Quantum Beam Science Directorate, Tokai, Japan*

**ABSTRACT:** This study develops a method for measuring the distribution of chloride concentration in concrete by Prompt Gamma-ray Analysis (PGA). PGA is a multi-elemental analysis technique based on nondestructive neutron technology. When the chloride concentration near the surface is known and its distribution profile is assumed by an error function, the distribution of the chloride concentration can be comparatively evaluated with good accuracy using PGA as already reported. However, under conditions such as rainfall or carbonation, the peak of chloride concentration is located at a certain depth inside the concrete and not near the concrete surface. To detect chloride concentrations at various depths below the surface, the present study proposes varying the incident angle of the neutron irradiation beam on the surface of the object. This method proves to be successful in measuring the arbitrary distribution of chloride concentrations in concrete.

## 1 INTRODUCTION

Japan has seen significant growth in the last fifty years in the construction industry. It has been reported that within the next several decades, 50% of residential buildings will be fifty years old or more (MLIT 2009). Considering such a forecast, efficient maintenance within the budget limits are needed, and the infrastructure management is shifting from corrective preservation to preventive preservation. Preventive maintenance is advantageous because detailed inspections are performed before the manifestation of deterioration, and appropriate measures are taken for maintaining the structure.

The corrosion of steel reinforcements by chlorides is of utmost concern in the degradation phenomena of concrete structures. Advanced chloride-induced deterioration is visually detected by the presence of corrosion cracks. To implement a preventive maintenance strategy, chloride ions have to be monitored in the concrete structures before cracks appear.

Steel reinforcement bars in concrete structures are protected from corrosion by passivating films, which form around the surface of steel reinforcement under alkaline conditions in concrete. However, when the threshold chloride ion concentration is exceeded, film depassivation occurs and active corrosion takes place through the fractured film. Therefore, for predicting the progress of chloride-induced

deterioration before the onset of reinforcement corrosion, it is essential to monitor the chloride ion concentration in concrete around steel reinforcement. The following outlines the currently used method for measuring the chloride ion content in concrete: Concrete cores are drilled from the structures and then divided into different sections corresponding to different depth profiles. Each section is powdered and the chloride ion content is determined from potentiometric titration measurements. This method is disadvantageous because it is time consuming and expensive; core drilling damages the building structure, and multiple core samples for repeated measurements cannot be taken at the same position in the structure.

The present study is a fundamental investigation necessary for the development of a non-destructive method to measure the distribution of chloride ion concentration in cover concrete via prompt gamma-ray analysis (PGA). PGA is a multi-elemental, non-destructive analysis technique. A nondestructive method for measuring the distribution of chloride ion concentrations in surface layers of concrete using PGA has been reported (Ujike et al., 2010). Using this method, the estimation of chloride concentration distribution in concrete is accurately determined when the chloride concentration gradually decreases from the surface. However, the estimation is poor when the chloride concentration is arbitrary and does not follow a decreasing trend. This study proposes a method of varying

the angle of neutron irradiation on the surface for measuring the arbitrary distribution of chloride ion concentrations.

## 2 EXPERIMENTAL METHODS

### 2.1 Prompt Gamma-ray analysis

Prompt gamma-rays are characteristic high energy gamma-rays emitted from a subject, when thermal neutrons are captured by the nucleus of the elements contained in the subject (Yonezawa 2003). In PGA, the prompt gamma-rays are detected by a radiographic detector. Because thermal neutrons with high transmission are irradiated, no pretreatment (such as powdering) of the sample material is required. The energy of the emitted prompt gamma-rays is dependent on the intrinsic energy of the processes occurring in the nucleus; therefore, many elements in the subject can be analyzed simultaneously according to the measurement of count by energy. Figure 1 is an example of prompt gamma-ray spectrum of concrete with chloride. The elements are analyzed quantitatively from position and height of the energy peaks. For example, the peak at 1163 keV in Figure 1 is due to chloride ions. The sensitivity to chloride ions is high using PGA; therefore, low concentrations, in the range of hundreds ppm, can be measured.

### 2.2 Equipment

In this study, the research reactor JRR-3 at Japan's Atomic Energy Agency (JAEA) was installed with PGA equipment. The neutron beam (flux 108 neutrons/cm<sup>2</sup>/s, width 5 mm) from the reactor is applied to the samples. Prompt gamma rays emitted from the sample are detected by a high-purity germanium detector, which is aligned perpendicular to the incident direction of the neutron beam.

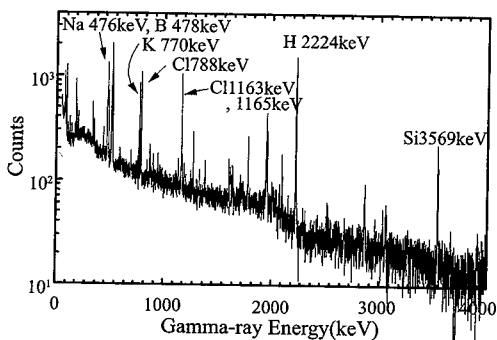


Figure 1. Example of gamma-ray spectrum of concrete with chloride.

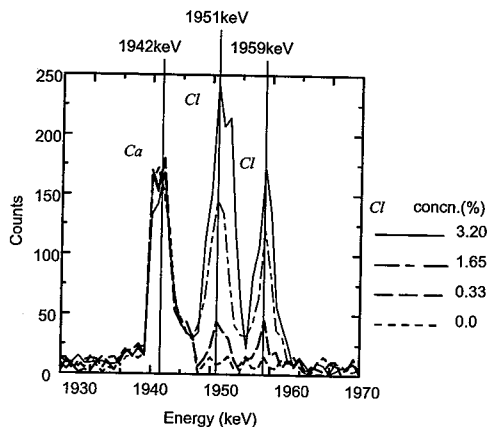


Figure 2. Gamma-ray spectrum near the object energy.

To quantitatively analyze the chloride ion concentration, the internal standard method was used in this study. Calcium was selected as the internal standard element, because it is present in cement in large amounts. The ratio of the counts for prompt gamma-rays for chloride to that of calcium was used as the index; hereinafter, it is referred to as the counting ratio. For this study, 1951 and 1942 keV are the energies of the prompt gamma-rays from chloride and calcium, respectively. The reactivity of these elements at these energies is relatively high, and because their prompt gamma-ray energies are close to each other, any fluctuations in prompt gamma-ray counts will affect both energies to the same extent. Figure 2 shows an example of the prompt gamma-ray spectrum near the energy of interest for this study. The counts for chloride at 1951 and 1959 keV increase with increasing chloride concentration in the concrete samples. However, the count for calcium at 1942 keV is almost constant. The fluctuations in the calcium gamma-ray count mainly depend on the amount of cement in the sample. For samples containing a large amount of aggregate, the peak counts for calcium and chloride decrease because of the decrease in the cement content in the sample. However, because we use the counting ratio, which remains constant in our analysis, PGA is advantageous in that no adjustment is necessary to account for varying aggregate contents in the samples.

### 2.3 Mortar boards

In this study, two types of mortar boards were used. Mortar boards with dimensions of 40 × 40 × 50 mm and made from Ordinary Portland cement and silica sand are used for examining the influence of the concrete mix with different water-cement ratio

and different sand-cement ratio on the prompt gamma-ray counts. The water-cement ratios were 40%, 50% and 60%. The sand-cement ratio was changed from 0% to 200%. The chloride concentration in the mortar boards was adjusted to 3 wt% of chloride to cement. This value is the amount of mixed-in chloride.

Another type of mortar board with dimensions of  $70 \times 30 \times 5$  mm and made from Ordinary Portland cement and silica sand was used for evaluating the arbitrary concentration distribution of chloride. The water-cement and sand-cement ratios were 40% and 100%, respectively. The chloride concentration in the mortar boards was varied from 0% to 3% in increments of 0.5%, and ten mortar boards were combined in a set. Figure 3 shows example of one set with ten mortar boards. An arbitrary concentration distribution was established by combining the boards with various chloride concentrations, because it is difficult to produce by penetration a concrete specimen with the arbitrary distribution of chloride ions in a short time. However, the chloride does not mix with all of five mortar boards from the sixth mortar board. For the PGA done in this study, the detectable range was adjusted to be the thickness of five mortar boards. The contributing gamma rays emitted from chloride ions contained in mortar boards beyond the fifth are defined as noise, because it has been reported that the chloride concentration calculated from the counting ratio varies at this depth and no reliable values are obtained (Ujike et al., 2010). Mortar boards without chloride ions are used in the sixth to tenth mortar boards for maintaining consistent experimental conditions. The following three cases were considered for the chloride concentration in the mortar boards:

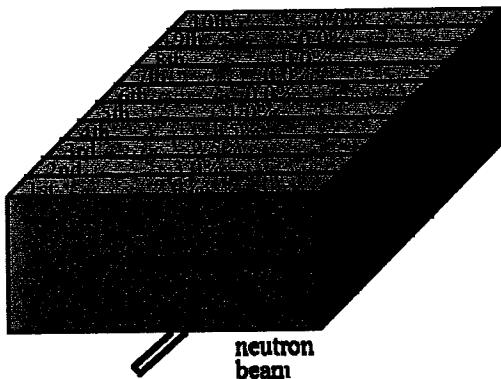


Figure 3. Example of combined mortar boards in a set.

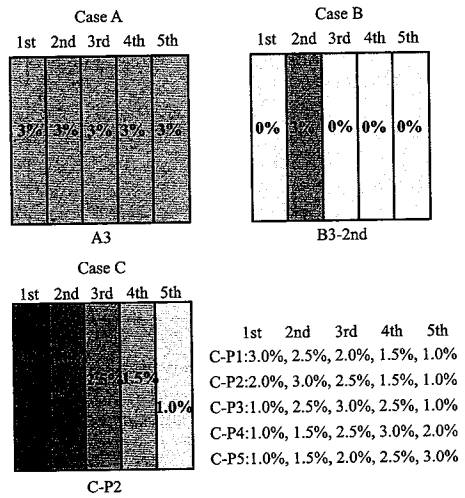


Figure 4. Combined chloride concentrations in the first to fifth mortar boards for Cases A–C.

Case A: All five mortar boards have the same chloride concentration.

Case B: Only one mortar board contains chloride; the other four contain no chloride.

Case C: The chloride concentration in each mortar board is mutually different.

Figure 4 shows examples of the combination of five mortar boards used in cases A, B and C, respectively. For case A, a numeral affixed to the letter A represents the chloride concentration in the mortar boards. For case B, the first number indicates the chloride concentration in a given mortar board while the second number indicates the position of the given mortar board. For case C, the sequential chloride concentration in all five mortar boards are given and the number attached to P indicates the position of the mortar board with the maximum chloride concentration.

### 3 RESULTS AND DISCUSSION

#### 3.1 Calibration curve for evaluating chloride concentrations

As shown in Figure 2, the gamma-ray counts for chloride increases and that for calcium is almost constant when the concentration of chloride ions in the mortar board increases, indicating that the counting ratio is proportional to the chloride concentration.

Figure 5 shows the counting ratio versus chloride concentrations for cases A and B. The proportionality constant (given by the slop of the lines in Figure 5) for case A is larger than those obtained

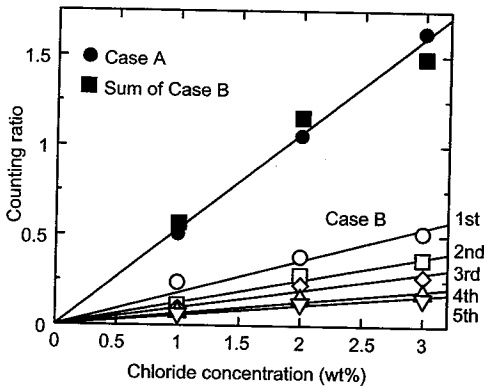


Figure 5. Relationship between chloride concentration and counting ratio.

for all case B combinations. Furthermore, in case B combinations, it is seen that the constant of proportionality decreases when the chloride mortar board is moved from the irradiated surface (first position) of the specimen to the opposite side (fifth position). This decrease is attributed to the fact that the number of neutrons reaching the fifth mortar board is less than the number impinging on the first mortar board because of absorption and scattering within the material. Thus, when evaluating the chloride concentration, it is necessary to consider the distance from the irradiated surface. And, black squares in Figure 5 are sum of the counting ratio of case B at each chloride concentration. As shown in Figure 5, the counting ratios of case A are in good agreement with the sum of the counting ratios for case B at each chloride concentration. That is, the principle of superposition consists between case A and case B. Thus, for evaluating the chloride concentration in concrete using PGA, we must consider a calibration curve that accounts for the mortar board position of the chloride.

As the number of transmitted neutrons decreases exponentially because of scattering and absorption in the material, the generation of prompt gamma-rays also decreases exponentially. The semi-log plot of Figure 6 shows the relationship between the counting ratio and the position of the mortar board that contains chloride. The straight lines in Figure 5 are regression lines expressed with the following equation obtained by a least squares method.

$$R = aC \cdot e^{-bd} \quad (1)$$

where,  $R$  is the counting ratio,  $C$  is the chloride concentration,  $d$  is the distance from the irradiation surface (i.e., distance from the irradiation

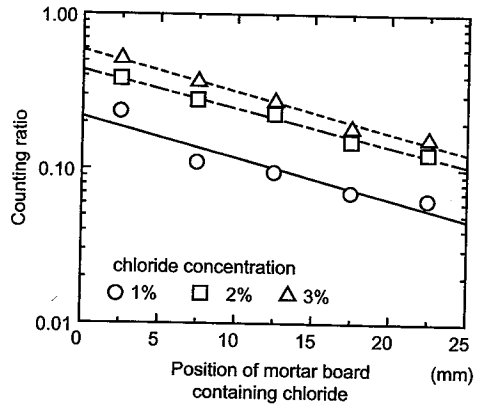


Figure 6. Effect of position of mortar board containing chloride on counting ratio.

surface to the center of the mortar board with chloride),  $a$  and  $b$  are regression coefficients, and  $aC$  is the counting ratio at position  $p = 0$ . Coefficient  $b$  gives the slope of the lines in Figure 6. Because the counting ratio is proportional to the chloride concentration, and if position  $p$  is constant, the straight lines in Figure 6 should be parallel. Although some data points are not on the lines, the regression lines in Figure 6 can be considered parallel for our purposes. The coefficients  $a$  and  $b$  depend on factors such as the neutron source, detector, and measuring time; therefore, these values have to be kept constant in a set of measurements. The calibration curves in Figure 6 are not dependent on the thickness of the mortar boards. If the calibration curve is obtained using a 2 mm mortar board, the evaluation of the chloride concentration at 2 mm intervals is performed as previously reported (Yamada, 2009).

### 3.2 Effect of mix proportions on counting ratios

The effect of varying the concrete mix on the counting ratios is examined. Figure 7 shows the effect of water-cement ratio on the counting ratio of chloride in mortar. The counting ratio hardly changes with varying water-cement ratios. Figure 8 shows the effect of sand-cement ratio on the counting ratio. In contrast, varying the sand-cement ratios (Figure 8) affects the counting ratio to a greater extent; however, the variation coefficient on the counting ratio is small at only 4.8%.

Because there are no significant differences in the counting ratios on varying the water-cement and sand-cement ratios, the effect of the concrete mix on the calibration curves is not significant. Therefore, samples with arbitrary water-cement and sand-cement proportions can be used for the calibration curves, and there is no problem in the

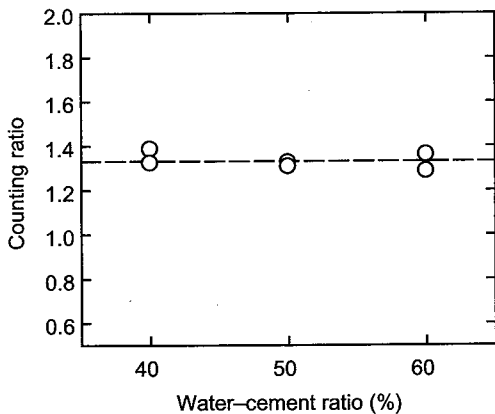


Figure 7. Effect of water-cement ratios on the counting ratio.

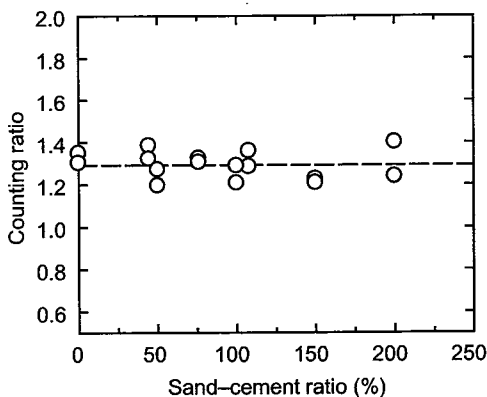


Figure 8. Effect of sand-cement ratios on the counting ratio.

application of the calibration curve for materials in which the concrete-mix proportions are unknown. However, when the limestone is used for the aggregate, this method of utilizing the calcium as the internal standard element cannot be used. For that case, the counts of chloride may be used directly in consideration of concrete mix.

### 3.3 Measurement of the distribution of chloride concentrations in samples

#### 3.3.1 Varying the irradiation angle

For the PGA in this study, the detectable range was adjusted to be the thickness of five mortar boards as mentioned above. We propose to evaluate the arbitrary chloride distribution by measuring gradual changes in the detectable range of prompt gamma-ray emission. As shown in Figure 9, the irradiation angle  $\theta$  of the neutron irradiation beam

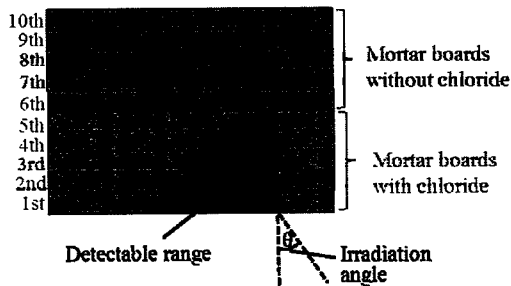


Figure 9. Irradiation angle changing method.

Table 1. Relationship between irradiation angle and detectable mortar boards.

Irradiation Angle	Distance from surface (mm)				
	2.5	7.5	12.5	17.5	22.5
80°	1st	1st	1st	1st	1st
65°	1st	1st	2nd	2nd	2nd
50°	1st	1st	2nd	3rd	3rd
35°	1st	2nd	2nd	3rd	4th
0°	1st	2nd	3rd	4th	5th

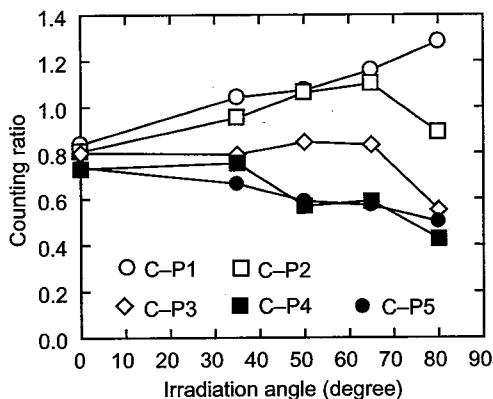


Figure 10. Change of counting ratio with the increase of the irradiation angle of neutron beam.

on the sample surface is gradually varied at 80°, 65°, 50°, 35°, 0°.

Table 1 shows the relationship between the irradiation angle and the detectable penetrable range, given by the depth in mm corresponding to the first to fifth mortar boards. The incident irradiation angle was set so that increments of one mortar board are incorporated into the detectable range with decreasing incident irradiation angle.

Figure 10 shows the change of the counting ratio with varying incident neutron irradiation angles.

The measured mortar boards were specifically combined because the position of mortar board with maximum chloride concentration is different. When the irradiation angle is 80°, the counting ratios of C-P3, C-P4 and C-P5 are almost the same values because only the first mortar board is in the detectable range, and the counting ratios of C-P2 and C-P1 are approximately twice and thrice this value, respectively. The relationship between them corresponds to the chloride ion concentration of the first mortar board. For C-P1, when the irradiation angle is reduced from 80°, the counting ratio decreases gradually with decreasing irradiation angle because the mortar boards with low chloride ion concentrations fall within the detectable range. Conversely, for C-P5, the counting ratio increases gradually with decreasing irradiation angle because the mortar board with high chloride ion concentration is detected. For C-P2, C-P3 and C-P4, when the irradiation angle is reduced from 80°, the counting ratio increases with decreasing irradiation angle until the mortar board with the maximum concentration of chloride is detected. This fact indicates that the position of the mortar board containing the maximum chloride ion concentration can be located by changing the irradiation angle.

### 3.3.2 Evaluation of the distribution of chloride concentrations in mortar boards

As illustrated in the previous section, on decreasing the incident irradiation angle, chloride concentrations at an increased depth below the surface can be detected. The evaluation of the chloride concentration of mortar boards is as follows.

At an irradiation angle of 80°, only the first mortar board is within the detectable range and the chloride concentration in the first mortar board is obtained from the measured counting ratio using the following equation:

$$C_1 = \frac{R_{80}}{\sum_{i=1}^5 a \cdot e^{-bd_i}} \quad (2)$$

$$= \frac{R_{80}}{a(e^{-2.5b} + e^{-7.5b} + e^{-12.5b} + e^{-17.5b} + e^{-22.5b})}$$

where  $C_1$  is the chloride concentration in the first mortar board,  $R_{80}$  is the measured counting ratio at irradiation angle 80°,  $d_i = 5i - 2.5$  (distance from surface to center of each mortar board), and  $a$  and  $b$  are the coefficients of the calibration curve.

At an irradiation angle of 65°, the chloride concentrations in the first and second mortar boards are detected. The chloride concentration in the first mortar board ( $C_1$ ) is a known from the measurement at an irradiation angle of 80°. The chloride

concentration in the second mortar board ( $C_2$ ) is calculated using the following equation:

$$C_2 = \frac{R_{65} - aC_1(e^{-2.5b} + e^{-7.5b})}{a(e^{-12.5b} + e^{-17.5b} + e^{-22.5b})} \quad (3)$$

where  $R_{65}$  is the measured counting ratio at an irradiation angle 65°.

Similarly, at irradiation angles 50°, 35° and 0°, the chloride concentration in the mortar boards are obtained using following equations (4), (5) and (6), respectively.

$$C_3 = \frac{R_{50} - aC_1(e^{-2.5b} + e^{-7.5b}) - aC_2e^{-12.5b}}{a(e^{-17.5b} + e^{-22.5b})} \quad (4)$$

$$C_4 = \frac{R_{35} - aC_1e^{-2.5b} - aC_2(e^{-7.5b} + e^{-12.5b}) - aC_3e^{-17.5b}}{ae^{-22.5b}} \quad (5)$$

$$C_5 = \frac{R_0 - a(C_1e^{-2.5b} + C_2e^{-7.5b} + C_3e^{-12.5b} + C_4e^{-17.5b})}{ae^{-22.5b}} \quad (6)$$

where  $C_3$ ,  $C_4$  and  $C_5$  are the chloride concentrations in third, fourth and fifth mortar boards respectively,  $R_{50}$ ,  $R_{35}$  and  $R_0$  are the measured counting ratios at irradiation angles 50°, 35° and 0°, respectively.

Figures 11–15 show the chloride concentration distribution obtained from varying the irradiation angle. As shown in Figures 11, 12 and 14, this method accurately determines the position of the mortar board containing the highest chloride concentration in C-P1, C-P2 and C-P4. The evaluated chloride concentrations for C-P1 and C-P2 agree qualitatively with the known concentrations. For C-P3 and C-P5 shown in Figures 13 and 15, respectively, although the peak position of the chloride concentration does not correspond to the correct mortar board, the distribution shape of the

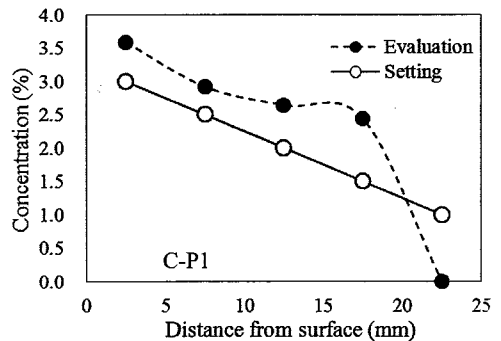


Figure 11. Evaluation of chloride concentration distribution in C-P1 by varying the detectable range.

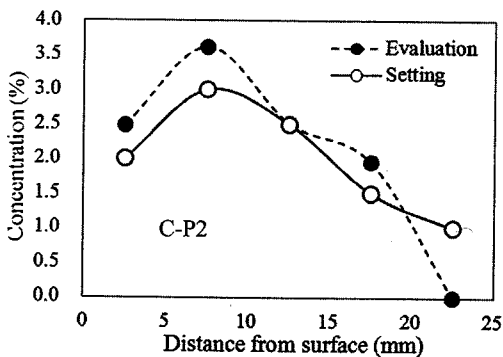


Figure 12. Evaluation of chloride concentration distribution in C-P2 by varying the detectable range (C-P2).

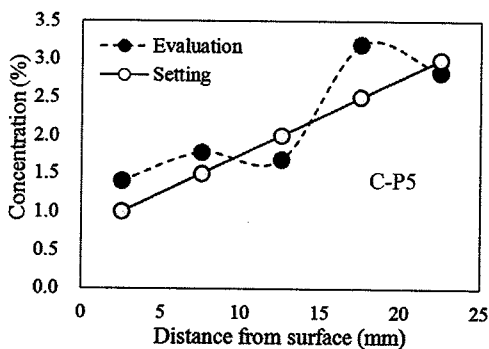


Figure 15. Evaluation of chloride concentration distribution in C-P5 by varying the detectable range.

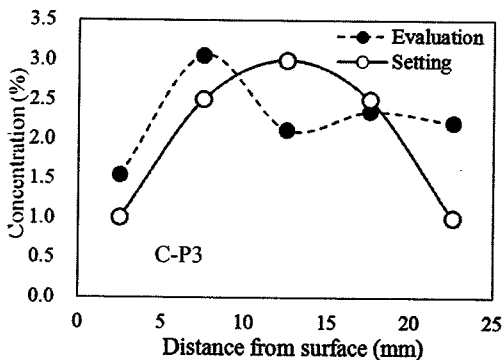


Figure 13. Evaluation of chloride concentration distribution in C-P3 by varying the detectable range.

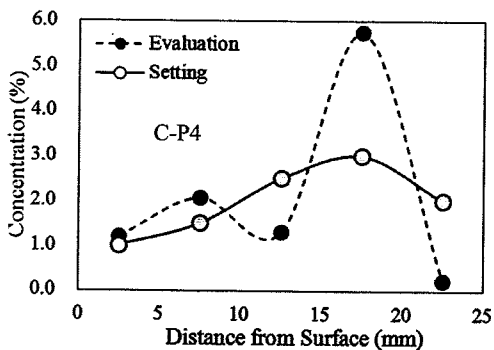


Figure 14. Evaluation of chloride concentration distribution in C-P4 by varying the detectable range.

chloride concentration roughly follows the correct trend.

The evaluated values on the first and second mortar boards are overestimated. Overestimating the chloride concentration on the first and/or second mortar boards can contribute to

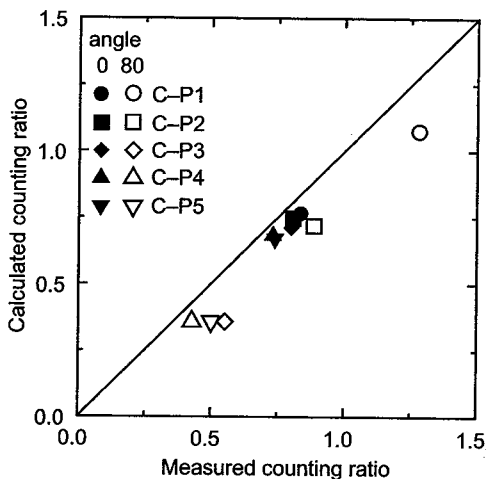


Figure 16. Comparison of measured counting ratios and calculated counting ratios at  $0^\circ$  (filled symbols) and  $80^\circ$  (open symbols).

underestimating the concentration on other mortar boards. The counting ratio calculated by the overestimated chloride concentration is subtracted from the measured counting ratio, as indicated in equations (4)–(6).

This overestimation mentioned above is caused by the noise generated outside the detectable range. Figure 16 shows the comparison of the measured counting ratio and the calculated counting ratio at the irradiation angles of  $0^\circ$  and  $80^\circ$ , respectively. The calculated counting ratio is the sum of the values calculated by substituting a set value for the chloride concentration of each mortar board into the calibration curve. The measured values are greater than the calculated values and the difference between measured and calculated values is more

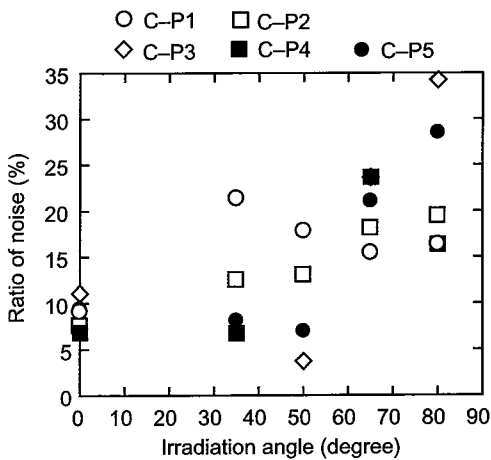


Figure 17. Effect of irradiation angle on noise.

remarkable in the case of irradiation angle 80°. As shown in Figure 9, there are mortar boards that contain chloride ions, which are undetected at the 80° irradiation angle measurement. The chloride ions outside the detectable range contribute to the noise and the noise is enlarged. The chloride concentration in the first mortar board is evaluated using equation (2). Because the measured counting ratio  $R_{80}$  contains noise, the chloride concentration in the first mortar board is overestimated.

Figure 17 shows the effect of the irradiation angle on the ratio of noise to the measured counting ratio. In this study, the difference between the measured counting ratio and the calculated counting ratio is defined as noise. The ratio of noise tends to increase with an increase in the irradiation angle roughly. Therefore, to improve the accuracy in evaluating the chloride concentration using the changing irradiation angle method, it is necessary to subtract the noise from the measured counting ratio appropriately.

#### 4 CONCLUSIONS

This study investigates the nondestructive measurement of the distribution of chloride concentrations by prompt gamma-ray analysis in combined mortar boards with different chloride ion concentrations. The following conclusions were drawn within the scope of the study.

1. The counting ratio of chloride to calcium is proportional to the chloride concentration and decreases exponentially with increasing depth from the surface.

2. The water-cement ratio and sand-cement ratio do not significantly influence the counting ratio; therefore, the calibration curve can be applied to different concrete mixes.
3. The position of the peak of chloride ion concentration can be determined by varying the irradiation angle.
4. Measuring arbitrary chloride ion distributions is possible by changing the neutron beam irradiation angle, although the resulting chloride ion concentration measured this way is overestimated in the vicinity of the surface.

Because the present study is a basic research to utilize the PGA for the non-destructive measurement of concrete structures, the neutron beam from the research reactor is used as neutron source. As a research in the future, it is necessary to examine the applicability of the proposal method in this study by using the portable neutron source like californium used in a previous study (Saleh 2000).

#### ACKNOWLEDGEMENTS

The authors would like to thank the Japan Society for the Promotion of Science for the financial support given by the Grant-in-Aid for Science Research, as a part of the present study. PGA in this study was carried out as the part of the shared facility use system of the Independent Administrative Institution Japan Atomic Energy Agency. The authors also thank JAEA for installing the PGA system.

#### REFERENCES

- Ministry of Land, Infrastructure, Transport and Tourism. 2009. *White Paper on Land, Infrastructure, Transport and Tourism in Japan 2009*.
- Saleh, H.H and Livingston, R.A. 2000. Experimental evaluation of a portable neutron-based gamma-spectroscopy system for chloride measurements in reinforced concrete. *Journal of Radioanalytical and Nuclear Chemistry*. Vol. 244, No. 2: 397–371.
- Ujike, I., Okazaki, S. Yamada, Y. and Matsue, H. 2010. A fundamental study on non-destructive measurement of chloride concentration in concrete by Prompt Gamma-ray Analysis, *proceedings of Sixth International Conference on Concrete under Severe Condition, Environment and Loading*: CD-ROM.
- Yamada, Y., Ujike, I., Okazaki, S. and Matsue, H. 2009. Study on non-destructive measurement of chloride concentration distribution in concrete by PGA. *Proceedings of the Japan Concrete Institute*, Vol. 31, No. 1: 1981–1986. (in Japanese).
- Yonezawa, C. 2002. Prompt  $\gamma$ -ray analysis with reactor neutrons. *Japan Analyst*, Vol. 51, No. 2: 61–96. (in Japanese).